Microstructure and microhardness in surface-nanocrystalline Al-alloy material

Y.G. Wei*, X.L. Wu, C. Zhu, M.H. Zhao
LNM, Institute of Mechanics, Chinese Academy of Sciences, Beijing 100080, China

Abstract

Discussed and analyzed are the surface-nanocrystallization of Al-alloy material manufactured by using the ultrasonic shot peening method. The transmission electron microscope (TEM) is used to examine the microstructure features and nanocrystalline mechanisms, such as, the formed microbands, the divided subbands, the infinitesimally divided and formed nanometer-sized grains and grain boundaries, etc. Based on the microscale observation and measurement, the mechanical behaviors of the surface-nanocrystalline Al-alloy material are investigated experimentally at submicron scale by means of the nano-indentation test. The load- and hardness-indent depth curves are measured. The grain size and its nonuniform effects are investigated. In the theoretical modeling, based on the microstructure characteristics and the experimental features, a dislocation pile-up model considering grain size effect based on the Mott theory is presented and used. The experimental hardness-indent depth curves which display the strong size, geometry and nonuniformity effects are successfully modeled and predicted.

Keywords: Surface-nanocrystalline Al-alloy; Microstructure; TEM observation; Nanoindentation test; Size effect.

1. Introduction

Recent studies have shown that the high strength nano-structured materials can be fabricated by using some special techniques. The severe plastic deformation (SPD) method can be used to fabricate the nanocrystalline (NC) materials [1-4]. In addition, the mechanical behaviors of the conventional materials can be improved by using some NC methods. The surface-nanocrystalline (SNC) technique can make the nanocrystallization within a material surface layer such that material behaviors can be improved considerably [5, 6]. The adopted SPD methods include: the large torsion method [1], the large pressing method [4], the ultrasonic shot peening (USP) method [5, 6], etc. The microstructure features of both the nano-structured bulk materials and the SNC materials have been widely investigated in [1-6]. Recent investigations have displayed that the SNC materials have the regular microstructures overall or locally within the SNC surface layer. The

* Corresponding author.
E-mail address: Ywei@LNM.imech.ac.cn (Y.G. Wei).

G.C. Sih (ed.), Multiscaling in Molecular and Continuum Mechanics: Interaction of Time and Size from Macro to Nano, 369–387.

variation of the representative cell size of the microstructures is from tens to hundreds of nanometers, even to microns from the NC surface to the interior of the material inside. The mechanical behavior of the NC materials has also been studied. Besides the works in [1-6], a wide characteristics of the NC materials have been investigated. They include the grain boundary behavior and plasticity in the NC Ni [7], the compressive behaviors of the NC Al-alloy [8], the surface roughness effect on the hardness of the NC Al-alloy [9], the grain rotation model of a 9-grain cluster mechanism for the NC copper [10], the strain-rate sensitivity in the NC Ni [11], the formed nanometer crystal grain due to indented for a bulk amorphous metal alloy [12], the tensile behaviors of the NC electrodeposited Ni [13] and the high tensile ductility of the NC copper [14]. Below the micron scale, the materials tend to display the strong size effects. Research along this line has been related to the nanoindentation tests for single crystal or coarse-grained metals [15-19]. The results show that indent depth decreases. The measured hardness curve displays an increasing trend, i.e., the size effect which has been explained by the strain gradient theories [20-25], the dislocation density theory [16, 9, 26], as well as the discrete dislocation theory [27]. The modeling and simulation results were consistent with the experimentally measured results. However, the NC materials are very complicated and quite different from the single crystal or coarse-grained materials. Besides the size effect, the influence of both the crystal grain size and grain shape distributions should affect the material mechanical behavior. This is because the NC material grain size is so small that it is comparable to the material length scale or the strain gradient sensitive zone size. Previous research on the nano-polycrystal Al and the thin film/substrate system [28], both the crystal grain size and the shape distribution effects were referred to as the "geometrical effect" so as to distinguish therm from the size effect described by the microscale parameter of the strain gradient theories. The microstructure cell model and the strain gradient plasticity theory have been studied with reference to the size and geometrical effect. The predicted and experimental results have been studied with reference to the effects of grain size and the microstructure characteristics in relation to the microscale parameter of the strain gradient theory [28]. Similar model has been used to investigate the size, geometry and nonuniformity effects in the SNC materials [29].

In what follows, the microstructure features in the SNC Al-alloy LC4 are first considered ked by using the USP method through transmission electron microscopy (TEM) and high resolution TEM (HRTEM) observation and measurement. Next, the mechanics behavior of the SNC Al-alloy material will be studied experimentally and theoretically based on the nanoindentation experiments. The specimens are designed and prepared according to the microstructure features of the NC material. The load- and hardness-depth curves are measured and analyzed. Using the Mott dislocation pile-up theory [30], a dislocation mechanism considering the grain boundary constraint effect will be presented and used to model the nano-indentation experiments for NC Al-alloy material as in [31]. Here, the attention will be focused on the microstructure observation, measurement and experiments. In addition, the material hardness curves will be predicted by using the model based on the Mott dislocation pile-up theory. Finally, through experimental research and the theoretical simulation and analysis for the SNC Al-alloy material, limitations and further work will also be discussed.

2. SNC Materials and Procedures

The procedures of the experimental specimen preparations are similar to those shown in [6] for another material, Al-alloy 7075. A brief description of the procedures is given as follows.

2.1 Material

The experimental material was a high purity Al-alloy LC4, with a composition (wt pct) of 2.5Mg, 5.6Zn, 0.4 Mn and 1.8Cu, balance Al. A commercially available plate was cut into pieces with $100 \times 100 \times 6$ mm^3 in dimension. A smooth surface finish was attained on the faces by polishing on 800-1200 grade SiC papers. Microscopic examination revealed an initial grain size of the order of ~80 microns.

2.2 The USP technique

The principle of the USP technique was described in [5]. A high-energy ultrasonic generator of high frequency (45 kHz) is used to vibrate the reflecting chamber by application of the stainless steel shots of 7.45mm diameter. The shots then performed repetitive, high-speed, and multi-directional impact onto the surface of the materials. Severe plastic strains were imparted into the surface by striking. The USP processing was conducted under vacuum at room temperature for 15 minutes. Through the USP technique treatment, the nano-scale crystal grains were formed near the NC surface, and the grain sizes change with the distance away from the NC (striking) surface in a gradient law, as described in the sketch figure, Fig. 1. Near the NC surface, nanometer-sized grains are formed. They also occur at the distance far away from the NC surface, for instance distance $D > 80$ micron. The grain size keeps the original coarse grain size. Between them, the grain sizes change with the distance away from the NC surface.

2.3 Microstructure examination

The JEM-2000FXII transmission electron microscope (TEM) operated at 200 kV was used for examination of the general microstructure features at low magnifications. A JEM-2010FEF high-spatial-resolution analytical electron microscope (HRTEM) is used for high magnifications and lattice image observations in grains with a focused beam having a diameter of ~1 nm. Lattice images were taken at close to the optimum defocus conditions, typically at a magnification of 500,000X, with the selected grain oriented close to <111> for lattice imaging. Thin TEM films were prepared by the steps: (1) sticking a castolite plate 2 mm thick on the peened surface, (2) cutting a bar 3 mm in diameter with the peened layer located at the middle, (3) cutting discs 30 micron thick using a diamond saw normal to the long axis of the bar and (4) dimpling and argon-ion-beam thinning to perforation at room temperature. This method allows the inspection of a well-identified depth of the processed surface layer. The grain size measurements were made directly from

TEM photomicrographs and the reported values are the averages from 40-60 individual measurements. Because of the elongated nature of the subgrains, the datum points were separately presented for measurements of the average of the short axis, the average of the long axis, and the average from randomly selected directions, whereas measurements for the grains were taken consistently along randomly selected directions.

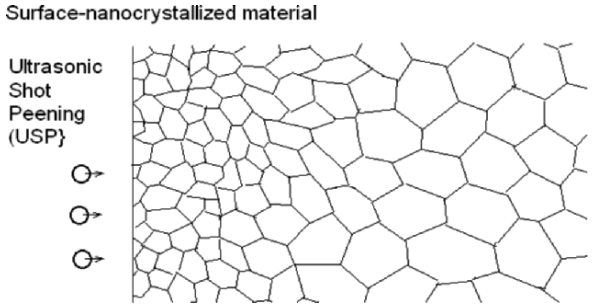

Fig. 1. Sketch of the surface-nanocrystallization principle for a coarse-grained metal undergoing the ultrasonic shot peening (USP) technique.

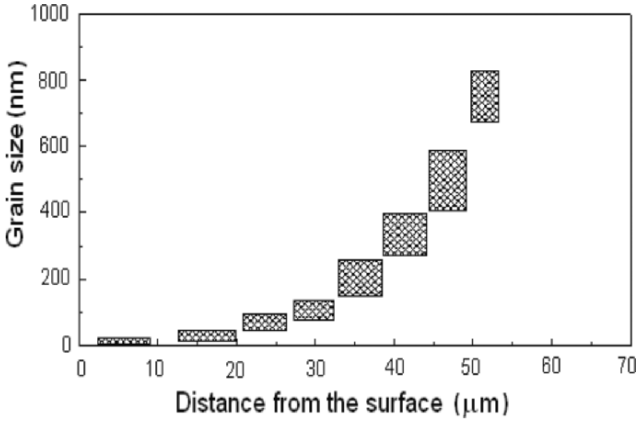

Fig. 2. Statistically averaging grain sizes changing with the distance away from the nanocrystalline(NC) surface of Al-alloy material.

3. Tem Observation and Measurement for SNC Al-alloy

3.1 Grain size distribution

Fig. 2 shows the relationship of the averaged grain size changing with distance away from the NC surface. According to the TEM observation and measurement, the original coarse grain size is kept at approximately 80 micron for distance larger than this. There the nanocrystallization effect seems to be negligible. From Fig. 2, the grains are nanocrystallized remarkably and the grain size attains the nanometer scale (grain size <100 nm) within a surface layer of ~30 micron thick. There exists

a big submicron grain region (100 nm – 1000 nm) within the region of distances, ~30 micron to ~60 micron.

3.2 TEM observation and analysis for microstructure of the SNC Al-alloy

To investigate the nanocrystallization mechanism of the SNC Al-alloy, a series of TEM micrographs are taken for a series of distances from the NC surface: 50 micron, 40 micron, 35 micron, 25 micron and 15 micron, respectively. These TEM micrographs record the microstructure features of the SNC Al-alloy corresponding to the given distances as shown in Figs. 3-7. Fig. 3(a) and 3(b) show the TEM photos taken at distances of 50 microns and 40 microns. From Figs. 3, the microbands are formed first within a micron scale grain region in Fig. 3(a), then the microband layers undergo a cut along another direction as the distance from the surface decreases slightly. The sub-bands are formed as shown in Fig. 3(b). Figs. 3(a) and 3(b) suggest that there exists a trend of forming the small-scale grains. With further decreasing of the distance away from the NC surface, the submicron scale grain sizes are formed as shown in Fig. 4. It can be concluded that for a continuous nanocrystallization process a coarse grain can be divided into a large numbers of the small-scale grains. Ths process can be further described as follows, (1) forming microbands, (2) dividing the microbands and forming the sub-bands and (3) dividing the sub-bands, etc. The number of the dividing steps is related to the distance away from the NC surface. Close to the NC surface, a coarse grain may undergo a large number of the dividing steps. And the very small scale grains (or nanometer grains) are formed. However, farther away from the NC surface, a coarse grain may undergo a small number of the dividing steps. The microbands or big size grains are attained. From Fig. 4, it can be observed that the grain sizes are nonuniform. This factor should be observable by microhardness testing. Even closer to the NC surface, the densely action of the nanocrystallization process gives rise to the formation of nanometer-sized grains as shown in Figs. 5 and 6. They show the formed nanometer-sized crystal grains corresponding to the distances D = 25 micron and D = 15 micron. The nanometer-sized crystal grains are formed through a considerably dividing process of the coarse grains during the nanocrystallization. Inset in Fig. 5 is the electron diffraction patterns, which indicate highly misoriented grain boundaries.

(a)

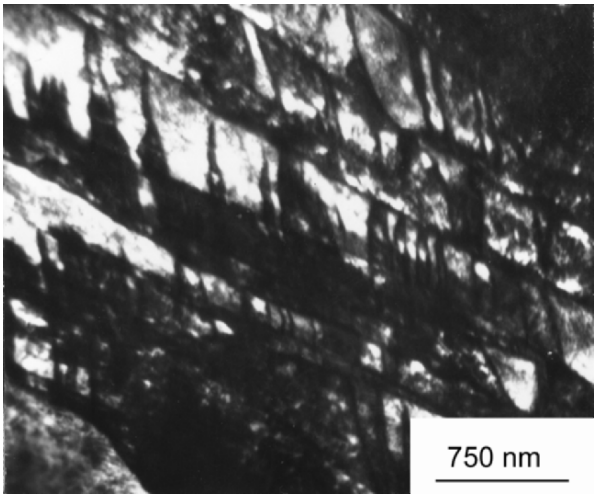

(b)

Fig. 3. TEM micrographs showing the layer microbands and subbands formed at the distances of D = 50 micron (a) and of D = 40 micron away from NC surface.

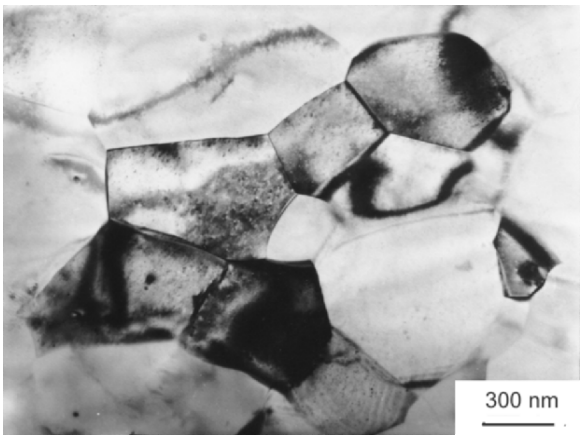

Fig. 4. TEM micrograph showing the formed submicron scale grain shapes at the distance of D = 35 micron away from the NC surface. Figure also shows that the formed grain sizes are non-uniform for given D.

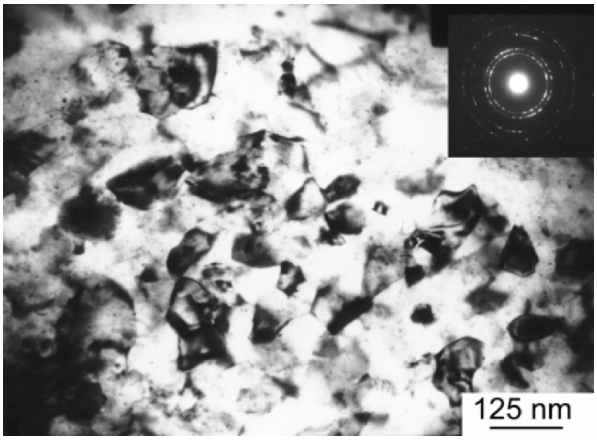

Fig. 5. Nanocrystal grains formed in nanocrystallization process (TEM photo), D = 25 micron. Inset is the electron diffraction pattern.

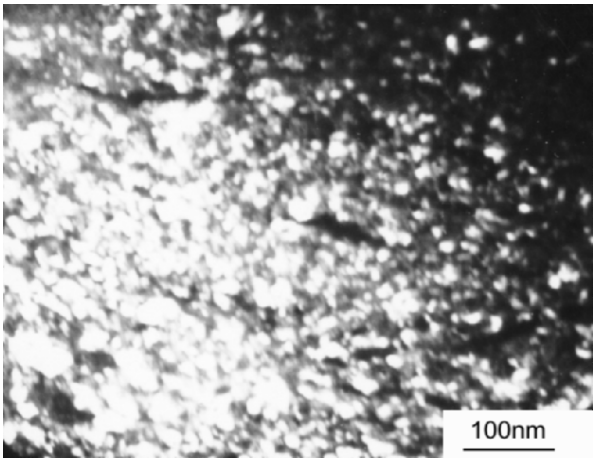

Fig. 6. TEM micrograph showing the formed nanometer-sized grains at distance D = 15 micron away from the NC surface.

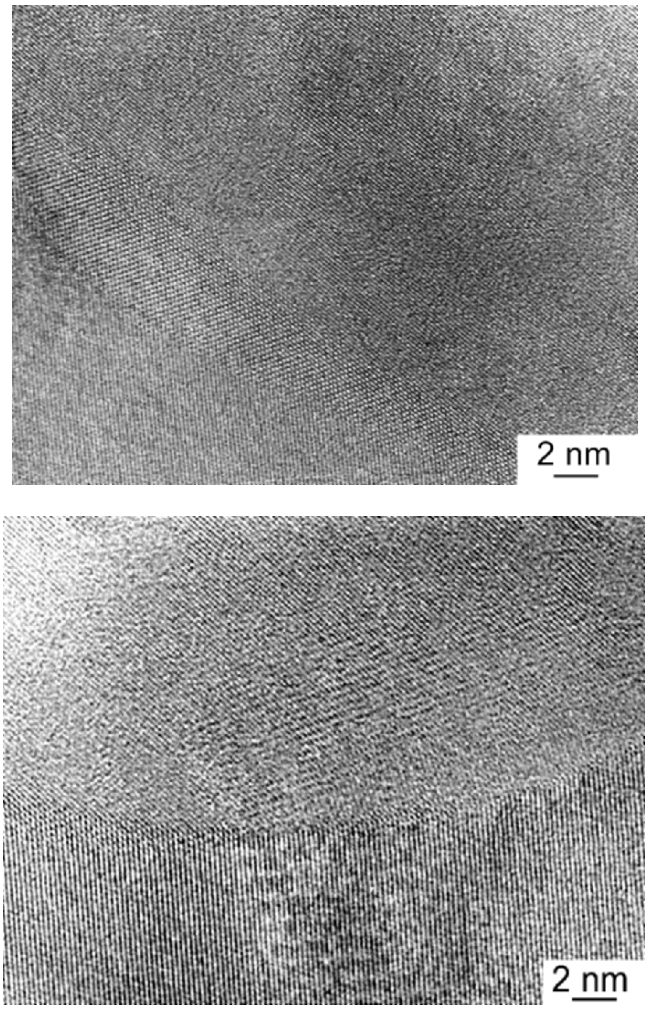

Fig. 7. HRTEM micrographs showing the formed nanometer-sized grains and grain boundary regions. (a) A grain boundary region is shown and its width is measured about 3~5 nanometer. (b) Joint of three nanometer-sized grains is shown.

In order to further examine the microstructure features of the formed NC material, Fig. 7 shows the HRTEM photos of the nanometer-sized grain and grain boundaries. At the nano-scale, a marked feature is that grain "boundary" is observed to be a "region" with a certain width. From Figs. 7(a) and 7(b) show the grain boundary geometry and measure the grain boundary thickness. For example, the grain boundary width is measured to be 3~5 nanometers. Fig. 7(b) shows a joint of three nanometer grains. The grain boundary region should occupy a high volume fraction in a nanometer-scale representative cell. The grain regions and grain boundary regions can be observed from Fig. 7. Moreover, from the HRTEM photos, the lattice of the NC material can be observed clearly.

4. Microhardness of the SNC Al-alloy Material

Nanoindentation test is considered as an effective method to reveal the mechanical behavior of the SNC materials.The corresponding load-indent depth curves and the microhardness curves can be measured. The resulting relations are closely connected to the mechanical behavior. For the SNC Al-alloy material, examine the grain size effect on the load- and hardness-indent depth curves.The indent points were randomly selected at the distance of 30 microns away from the NC surface, where the average grain size is about 200 nm from the TEM measurement. Indentation direction was normal to the NC surface. The specimen surfaces were polished first, then nano-indentation experiments were performed. It is worth noting that for the NC materials the indenter tip is probably located at a grain boundary region. Hence, the measured experimental data may deviate from the main trend of the experimental results. However, for t = 200nm, there is a great possibility of the indenter tip being located at the grain region, because the grain region is much larger than the grain boundary region. The prevailing instrument is the MTS-Nanoindenter-XP. The nano-indentation test method is called the continuous stiffness method, i.e., the load- and hardness-depth curves are measured through continuously increasing the indent loading for a fixed point.

Figure 8 shows the measured load- and hardness-depth curves for several selected loading points. From Fig. 8(a), the load-depth curves seem to have a good reproducibility. Several curves based on several indentations are close to each other. However, from Figs. 8(b) and 8(c), there exists a big deviation among the hardness-depth curves, which strongly depend on the loading points. This effect appears to be contributed by grain size nonuniformity, Fig. 4. The submicron scale grain size effects in Figs. 8(b) and 8(c) are caused by grain size non-uniformity. The differences between the measured hardness values based on different indentations are large. However the differences decrease with increasing the indent depth. For comparison, the nano-indentation experiments were performed for the coarse-grained case by selecting the loading points at a distance of 100 microns bring far away from the NC surface where the, grain size equals to ~80 microns. The measured load- and hardness-depth curves are plotted in Figs. 9(a) and (b) where the results of the coarse-grained size results are compared with those of the nanocrystalline grain shown in Fig. 8. The load- and hardness-depth curves of the coarse-grained results have much better reproducibility. However, the load- and hardness-depth values of the NC materials are much higher than those of the corresponding coarse-grained materials.

5. Mechanism Characterization and Analysis

Materials display the size effect in the submicron- or nanometer-scale [15-19]. Several theories have been presented and used to explain these size effects. They include the strain gradient theories [20-25], dislocation density theory [16, 9, 26] and discrete dislocation theory [27]. The indentation size effect for single crystal materials or for coarse-grained materials has been subject to many studies.

However, for the NC or SNC materials, the corresponding studies are very few [11,12]. In addition to the size effect described by the length parameters in the theories such as the strain gradient plasticity theory, there is an additional length scale of the grain size. In these cases, the grain size is so small that it is comparable to the material length scale parameter. The study of the combined effects is important for understanding the mechanical properties of nanometer materials. The dislocation density model based on the Taylor theory has been widely and successfully used to model the indentation size effect for single or coarse crystals. Since the grain size is comparable to the characteristic length scale of dislocation density, the grain boundary constraint can be considerable. Therefore the dislocation density model based on the Taylor theory has failed to describe the case. The dislocation density model based on the Mott theory [30] is used to model the mechanical behaviors of the SNC materials. The load- and hardness-depth curve behavior has been in earlier discussions.

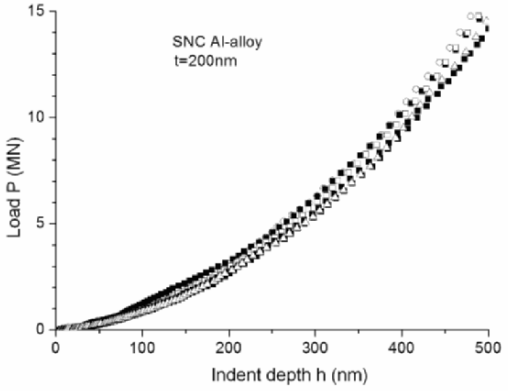

(a)

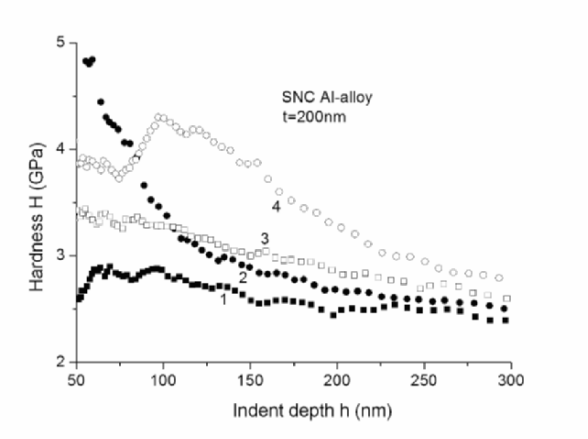

(b)

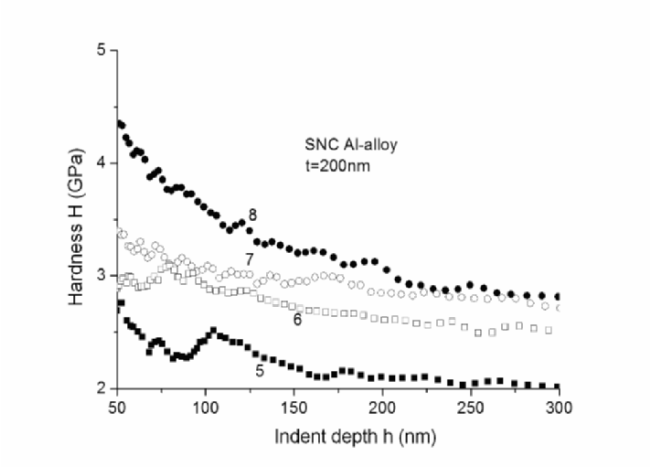

(c)

Fig. 8. Variations of load and microhardness with indent depth for SNC Al-alloy material. (a) Load-indent depth curves for several load points. (b) and (c) Hardness-indent depth curves for different load points. (b) for one group of four load points and (c) for another group of four load points.

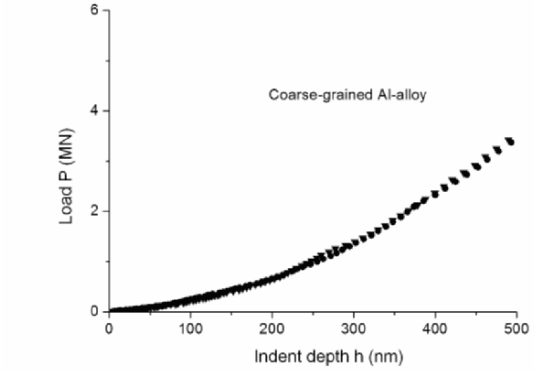

(a)

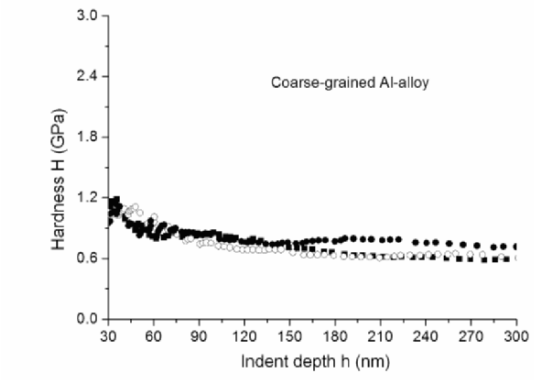

(b)

Fig. 9. Variations of load and hardness with indent depth for the coarse-grained Al-alloy material. (a) Load-indent depth curves for several load points. (b) Hardness-indent depth curves for several load points.

5.1 Dislocation density model based on the Taylor theory

Review first the formulas of the dislocation density model based on the Taylor theory. The nano-indentation test for metals belongs to the case of the nonuniform plastic strain problem. From the dislocation density theory, the dislocation density is also nonuniform which can be divided into two parts They are the statistically stored dislocation density and the geometrically necessary dislocation density [32, 33]. In this case, the dislocation density depends not only on the applied load, but also on the microstructure geometrical parameters. The geometrically necessary dislocation density depends on the geometrical parameters. For the nano-indentation test problem, a deformation-permitted dislocation mechanism is assumed to prevail., Obtained in [16] is a simple and an approximate relation for the total dislocation density, $\rho_T = B(1+h^*/h)$. This depends on the indent depth h. Putting together the related relations involving the Taylor model relation, Mises flow criterion, Tabor factor relation and above dislocation density relation, there results

$$\tau = \alpha\mu b\sqrt{\rho_T}\ , \rho_T = B(1+h^*/h)\ , \sigma = \sqrt{3}\tau\ , H = 3\sigma \tag{1}$$

where τ and σ are the shear flow stress and Mises effective flow stress, respectively. Note that μ is the shear modulus, b the Burger's vector and α a geometrical constant equal to about 0.3. The constants B and h^* are determined from the nano-indentation test. B is statistically stored dislocation density and. h^* is a characteristic length describing the varying strength of the geometrically necessary dislocation density or being related to the strain gradient dominated zone size [9]. For $h < h^*$, the geometrically necessary dislocation density prevails. Otherwise, the statistically stored dislocation density prevails. From Eq. (1), It is found that [16]

$$H = H_0\sqrt{1+h^*/h} \tag{2}$$

Where

$$H_0 = 3\sqrt{3}\alpha\mu b\sqrt{B} \tag{3}$$

Here, H_0 is the macroscale hardness without considering the size effects. Its value can be determined by Eq. (2) for modeling material hardness of a deep indentation, i.e., for large value of h. The hardness-depth relationship based on the Taylor theory in Eq. (2), is simple and effective for describing the situation case where the dislocation pile-up is caused by grain boundary constraint. There are two parameters in the model, (H_0, h^*), by which the hardness-depth relationship for single crystal metals and for coarse-grained metals can be effectively characterized. When the effect of the geometrically necessary dislocation density can be neglected. This correspond to a deep indentation problem (small h^* or large h) where the hardness is a constant such that H_0 is only related to the macroscale parameters of the material [34, 35].

5.2 Dislocation density model based on the Mott theory

For a NC material, the grain size is comparable to the characteristic length scale of dislocation density. Then the grain boundary constraint effects can be considerable. Within an indented grain region, load increase will nucleate dislocations which move and pile-up near grain boundaries. According to Mott theory [30], the corresponding shear flow stress within a material can be described as

$$\tau = \frac{1}{2\pi}\mu(nb)\sqrt{\rho_T} \tag{4}$$

where n is the number of the piled-up dislocations along a single edge dislocation plane. ρ_T is the total dislocation density of the super-dislocation with the Burgers vector nb. Similarly, ρ_T is divided into the statistically stored dislocation density and the geometrically necessary dislocation density. In order to find the geometrically necessary dislocation density, consider a model to describe the deformation mechanism of the super-dislocations in the nan-oindentation test, as

shown in Fig. 10. For simplicity assuming that the indenter tip will not penetrate into the grain boundaries. In the Fig. 10, t is the representative grain size in the indenting direction. Note that the volume occupied by the super-dislocations is assumed to be a part of the semi-sphere due to the grain boundary constraint, similar to the derivation in [16] that leads to

$$H = \bar{H}_0\sqrt{1+(h^*/t)F(h/t,\ \theta)} \tag{5}$$

Where

$$\bar{H}_0 = \frac{3\sqrt{3}}{2\pi}\mu(nb)\sqrt{B}\ , \tag{6}$$

And

$$F(\frac{h}{t},\ \theta) = \begin{cases} 1/[(h/t)(1-\frac{1}{2}\tan\theta)], & h/t < \tan\theta; \\ (h/t)^2/[\frac{3}{2}(h/t)^2\tan\theta - \frac{1}{2}\tan^3\theta - \frac{1}{2}(h/t)^3\tan\theta], & h/t \geq \tan\theta \end{cases} \tag{7}$$

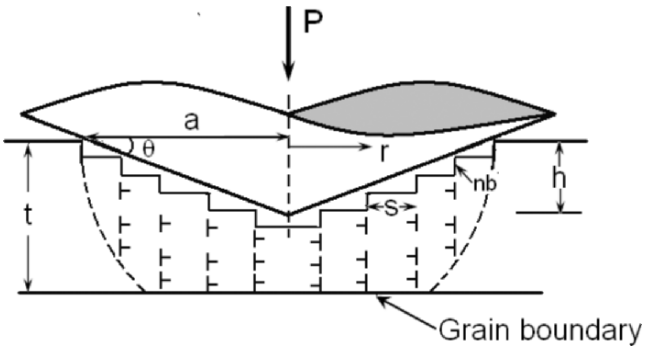

Fig. 10. Super-dislocation deformation mechanism in nanoindentation test based on the Mott theory [30].

In Eq. (6), B is the statistically stored dislocation density of the super-dislocations. The nano-indenter angle $\theta \approx 15^o$ for the tip is used in the present experiments. In deriving Eq. (7), for $h/t \geq \tan\theta$, the adopted volume in

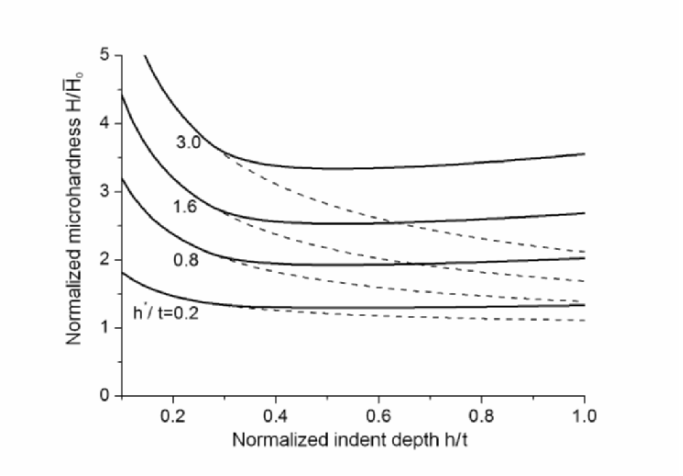

(a)

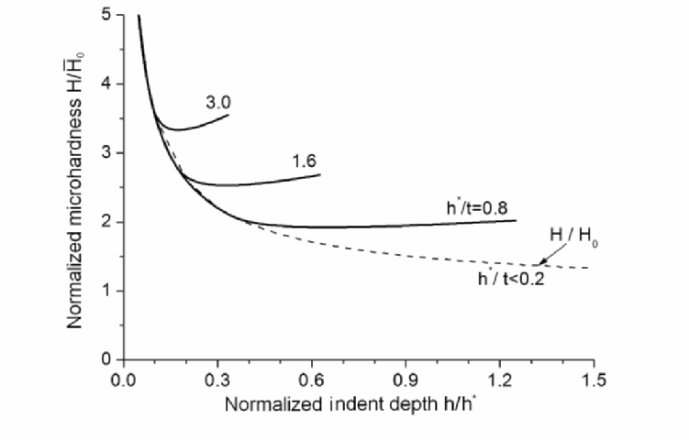

(b)

Fig. 11. Variations of normalized hardness with the normalized indent depth for several grain size values based on the present model. (a) Grain size as normalizing quantity, (b) h* as normalizing quantity. Solid lines stand for using the present model, and dashed lines stand for using the Taylor model.

calculating the geometrically necessary dislocation density is only a part of the semi-sphere in Fig. 10, instead of a complete semi-sphere as adopted in [16] for application of the Taylor model to a uniform material. Differing from the derivation

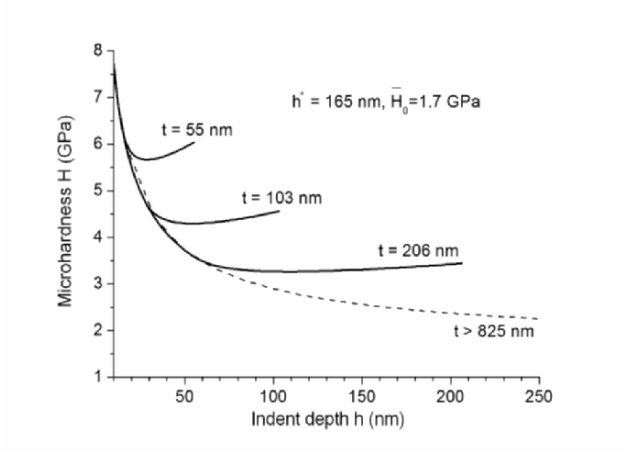

(c)

Fig. 12. Microhardness modeling for the SNC Al-alloy material by using the present model. Hardness-depth curves are grain-size sensitive.

and results in [16, 31] for the volume calculation of the dislocation region, the indenter volume was deducted in the present research. Comparing Eqs. (3) and (6), $\bar{H}_0$ is usually larger than H_0 because the piled-up dislocation number n is a large number [30, 31]. There are three parameters the Mott theory, $(\bar{H}_0, h^*, t)$ where t is the representative grain size in the direction of indentation. Examination of the present model (Fig. 10) suggests that it may be ideal for describing the case where the grain boundary constraints on the indented grain are strong in normal direction and weak in tangential direction. The case of weak constraint along the direction of the grain boundary seems suitable for a thin film/substrate system subject to nano-indentation along the normal direction of the thin film [35].

5.3 Modeling the microhardness of the SNC material

The hardness-depth relationships of the NC materials based on the present model are plotted in Figs. 11. Fig. 11(a) shows the curves of $H/\bar{H}_0 \sim h/t$ for several values of h^*/t. The hardness increases with decreasing indent depth. However, when indent depth is larger than a certain value, then the reverse trend is obtained. This conclusion differs from the case when the indenter volume is not deducted in calculating the volume of dislocation region [31], where the indent depth increases with the hardness-depth curves tending to stable values described by

$$H/\bar{H}_0 \approx \sqrt{1+(h^*/t)/(\tfrac{3}{2}\tan\theta)} \tag{8}$$

For comparison, the Taylor theory results are also shown in Fig. 11 for several h^* values. Refer to the dashed lines where t can be understood as any reference

length. The hardness curves based on the Taylor theory decreases as the indent depth increases. When the indent depth tends to infinity, $H/\bar{H}_0$ tends to unity. On the other hand, for h^* fixed the hardness increases with decreasing grain size (t). Fig. 11(b) shows the relationships of $H/\bar{H}_0 \sim h/h^*$ for several values of h^*/t. For comparison, the curve based on the Taylor theory is also plotted as dashed line. From Fig. 11(b), the hardness increases as the grain size decreases. As grain size increases, the hardness curve tends to a stable value depending on the grain size values. The hardness curve from the Taylor theory is independent of the grain size. From Fig. 11(b), when grain size (t) is large enough, say $h^*/t < 0.2$, the results based on both the Mott theory and the Taylor theory agree

Modeling of the experimental results of the SNC Al-alloy shown in Fig. 8, there results the hardness-depth curves in Fig. 12 for the average grain size $t = 200$ nm, length scale $h^* = 165$ nm [9] and $\bar{H}_0 = 1.7$GPa. Comparing the results in Fig. 12 and the experimental results in Fig. 8, the simple model developed is found to capture the complicated microhardness features of the SNC Al-alloy LC4.

6. Concluding Remarks

The microstructure features of the SNC Al-alloy LC4 have been observed and measured by using the TEM technique. The surface-nanocrystallization mechanism has been analyzed. Using the USP method for the surface-nanocrystallization of the Al-alloy LC4 at the distance far away from the NC surface, the original coarse grains were cut and the microbands with a multilayer feature were formed. With decreasing distance, the microbands were subdivided into many small pieces. Close to the surface, the micron or submicron scale grains were produced. At the distance very close to the NC surface, the nanometer-sized grains were produced.

The mechanical behavior of the SNC Al-alloy material has been investigated from both experimental and theoretical perspectives. The nano-indentation experiment has been performed at the distance where the grain size is in the submicron scale ($t = 200$ nm) and the hardness-depth curves have been measured. The nano-indentation experimental results have displayed. They show that the hardness of the original Al-alloy polycrystal material has been improved considerably. The theoretical research involves combining the observed microstructure features of the NC material and the characteristics of the nano-indentation experiments. A dislocation pile-up model has been presented to model the experimental hardness curves. The modeling results are roughly consistent with experimental measurements.

TEM observations for the SNC Al-alloy material microstructure show that near the NC surface the grain size is very small (several nanometers). The grain boundary region occupies a high volume fraction in a representative cell of the NC material. The dislocation pile-up model adopted in the present research for nano-indentation test should be revised to consider the effects of the grain rotation and grain boundary separation in tangential direction. In order to investigate the

mechanical behavior of the SNC material near the NC surface, some more reasonable and effective microscopic theory still needs to be explored in the future.

Acknowledgements

This work was supported by the National Natural Science Foundation of China through Grants 10432050 and 10428207.

References

[1] Valiev RZ, Korznikov AV, Mulyukov RR, Structure and properties of ultrafine-grained materials produced by severe plastic deformation. Materials Science and Engineering A 168: 141, 1993.
[2] Valiev RZ, Ivanisenko YV, Rauch EF, Baudelet B, Structure and deformation behavior of armco iron subjected to severe plastic deformation. Acta Mater. 44: 4705, 1996.
[3] Valiev RZ, Islamgaliev RK, Enhanced superplasticity of ultrafine-grained alloys processed by severe plastic deformation. Materials Science Forum 304: 39, 1999.
[4] Valiev RZ, Islamgaliev RK, Alexandrov IV, Bulk nanostructured materials from severe plastic deformation. Progress in Materials Science 45: 103, 2000.
[5] Lu K, Lu J, Surface nanocrystallization (SNC) of metallic materials-presentation of the concept behind a new approach. J Mater. Sci & Tech. 15: 193, 1999.
[6] Wu X, Tao N, Hong Y et al. Microstructure and evolution of mechanically-induced ultrafine grain in surface layer of Al-alloy subjected to USSP. Acta Mater. 50: 2075, 2002.
[7] Shan Z, Stach E, Wiezorek J et al., Grain boundary-mediated plasticity in nanocrystalline nickel. Science 305: 654, 2004.
[8] Wei Y, Zhu C, Wu X, Micro-scale mechanics investigations of the surface-nanocrystalline Al-alloy material. Science in China (Series G) 47: 86, 2004.
[9] Wei Y, Wang X, Zhao M, Size effect measurement and characterization in nanoindentation test. J. Mater. Res. 19: 208, 2004.
[10] Yang W, Wang H, Mechanics modeling for deformation of nano-grained metals. J. Mech. Phys. Solids 52: 875, 2004.
[11] Schwaiger R, Moser B, Dao M, Chollacoop N, Suresh S, Some critical experiments on the strain rate sensitivity of nanocrystalline nickel. Acta Mater. 51: 5159, 2003.
[12] Kim J, Choi Y, Suresh S, Argon AS, Nanocrystallization during nanoindentation of a bulk amorphous metal alloy at room temperature. Science 295: 654, 2002.
[13] Torre F, Swygenhoven HV, Victoria M, Nanocrystalline electrodeposited Ni: microstructure and tensile properties. Acta Mater. 50: 3957, 2002.
[14] Wang Y, Chen M, Zhou F, Ma E, High tensile ductility in a nanostructured metal. Nature 419: 912, 2002.
[15] Ma Q, Clarke DR, Size dependent hardness of silver single crystals. J. Mater. Res. 10: 853, 1995.
[16] Nix WD, Gao H, Indentation size effects in crystalline materials: a law for strain gradient plasticity. J. Mech. Phys. Solids 46: 411, 1998.
[17] McElhaney KW, Vlassak JJ, Nix WD, Determination of indenter tip geometry and indentation contact area for depth-sensing indentation experiments. J. Mater. Res. 13: 1300, 1998.
[18] Wei Y, Wang X, Wu X, Bai Y, Theoretical and experimental researches of size effect in micro-indentation test. Science in China (Series A) 44: 74, 2001.
[19] Zhang TY, Wu WH, Zhao MH, The role of plastic deformation of rough surfaces in the size-dependent hardness. Acta Mater. 52: 57, 2004.
[20] Fleck NA, Hutchinson JW, Strain gradient plasticity. Advances in Applied Mechanics 33: 295, 1997.

[21] Gao H, Huang Y, Nix WD, Hutchinson JW, Mechanism-based strain gradient plasticity-I. Theory. J Mech Phys Solids 47: 1239, 1999.
[22] Chen S, Wang TC, A new hardening law for strain gradient plasticity. Acta Mater. 48: 3997, 2000.
[23] Wei Y, Hutchinson JW, Steady-state crack growth and work of fracture for solids characterized by strain gradient plasticity. J. Mech. Phys. Solids 45: 1253, 1997.
[24] Begley M, Hutchinson JW, The mechanics of size-dependent indentation. J Mech Phys Solids 46: 1029, 1998.
[25] Wei Y, Hutchinson JW, Hardness trends in micron scale indentation. J. Mech. Phys. Solids 51: 2037, 2003.
[26] Swadener JG, George EP, Pharr GM, The correlation of the indentation size effect measured with indenters of various shapes. J. Mech. Phys. Solids 50: 681, 2002.
[27] Cleveringa H, Gissen E, Needleman A, A discrete dislocation analysiss of bending. Int. J. Plasticity 15: 837, 1999.
[28] Wei Y, Wang X, Zhao M, Cheng CM, Bai YL, Size effect and geometrical effect of solids in micro-indentation test. Acta Mechanica Sinica 19: 59, 2003.
[29] Wei Y, Shu S, Du Y, Zhu C, Size, geometry and nonuniformity effects of surface-nanocrystalline aluminum in nanoindentation test. Int. J. Plasticity 21: 2089, 2005.
[30] Mott NF, The theory of the properties of materials. Phil. Mag. 43: 1151, 1952.
[31] Wei Y, Chen X, Shu S, Zhu C, Nonuniformity effect of surface-nanocrystalline materials in nanoindentation test. Int. J. for Multiscale Computational Engineering, 2005. (In press)
[32] Ashby MF, The deformation of plastically non-homogeneous material. Philos. Mag. 21: 399, 1970.
[33] Fleck NA, Muller GM, Ashby MF, Hutchinson JW, Strain gradient plasticity theory and experiment. Acta Metall. Mater. 42: 475, 1994.
[34] Cheng YT, Cheng CM, Scaling relationships in conical indentation of elastic-perfectly plastic solids. Int. J. Solids Structures 36: 1231, 1999.
[35] Kriese MD, Gerberich WW, Moody NR, Quantitative adhesion measures of multilayer films: Part I: indentation mechanics. J. Mater. Res. 14: 3007, 1999.